



**Fermi National Accelerator Laboratory**

**FERMILAB-Pub-96/262**

**Analyses and Simulations of Longitudinal Motion  
in  $\mu$ -Recirculating Linacs**

D. Neuffer

*Fermi National Accelerator Laboratory  
P.O. Box 500, Batavia, Illinois 60510*

August 1996

Submitted to *Nuclear Instruments and Methods*

# Analyses and Simulations of Longitudinal Motion in $\mu$ -Recirculating Linacs

David Neuffer, Fermilab, P. O. Box 500, Batavia IL 60510

## Abstract

We present an analysis of the acceleration scenario for a high-energy  $\mu^+\mu^-$  collider. Acceleration from GeV to TeV energies is required, accompanied by bunch compression to collider-scale bunch lengths. The baseline scenario is a cascade of recirculating linacs (RLAs), with each linac increasing the beam energy by an order of magnitude. Bunch compression can occur both in the linacs themselves and in the transports connecting linacs. Constraints on acceleration design are discussed, and possible scenarios are developed. A simulation tool for RLA acceleration is presented and simulations of acceleration are described. Wakefield effects are included. Implications for  $\mu^+\mu^-$  collider scenario development are discussed, and directions for further studies are indicated.

## Introduction

Recently, investigation of the concept of  $\mu^+\mu^-$  colliders has intensified.<sup>1, 2, 3</sup> In this concept a hadronic accelerator produces large numbers of  $\pi$ 's, which produce  $\mu$ 's from  $\pi$ -decay. The  $\mu$ 's are collected and cooled, and then accelerated to collisions in a collider ring. Table 1 displays parameters of a possible collider system. In this note we study the  $\mu$ -acceleration scenario, in which the muons are accelerated from GeV to TeV energies. As previously discussed,<sup>4</sup> various scenarios for acceleration can be considered (linac, rapid-cycling synchrotron, and recirculating linac), which can accelerate muons to full energy within the limits of the  $\mu$  lifetime. Of these scenarios, the recirculating-linac based scenarios appear to be most readily attainable with current technology, and the recirculating linac appears well matched to the limited  $\mu$  lifetime.

In a recirculating linac (or RLA), the beam is injected, accelerated and returned for several passes of acceleration in the same linac(s), with a separate return path for each pass (see Fig. 1). At the end of a linac, the beam passes through dipoles, which sort the beam by energy, directing it to an energy-matched return arc. The various energy transports are then recombined at the end of the arc for further acceleration in the following linac. At each turn the beam passes into a higher-energy arc until full energy is reached, when the beam is transferred to another linac or the collider.

The RLA permits economic reuse of an expensive accelerating structure for several turns of acceleration. Since the beam passes through a separate transport on each turn, the magnets can be at fixed-field, allowing superconducting magnets, and simplified designs. However since each turn requires a separate return transport, cost and complexity considerations limit the number of turns to a finite number ( $\sim 10$ — $20$ ), which is also well-matched to the limited  $\mu$  lifetime (see below).

Because of the independence of each return transport, there is an enormous flexibility in RLA design, with only the rf acceleration frequency and voltage remaining constant from linac pass to linac pass. Since return path lengths are independent, the synchronous phase  $\phi_s$  can be changed from pass to pass. Also the chromicity,  $M_{56} = \partial z / \partial(\delta p/p)$ , where  $z$  is particle position within the bunch, can be changed from turn to turn, by fitting the transport. Higher order chromicity control ( $M_{566}$ ) with sextupoles is also possible, and one can consider adding higher-harmonic rf. This flexibility is however constrained by the beam dynamics requirements and by cost/complexity considerations.

In this paper, we study the acceleration scenarios in further detail. We first discuss the acceleration requirements, from which we develop candidate scenarios. An optimum scenario would appear to be a sequence of RLA's of increasing size, rf voltage, rf frequency and peak energy. The scenarios include bunching between RLA's, which reduces bunch lengths to match the higher frequency rf and to meet collider requirements. Scenarios with 3 or 4 RLA's are developed. A simulation tool called  $\mu$ RLA is described and used to explore beam dynamics within recirculating linac (RLA) acceleration scenarios. Conclusions and directions for further studies are developed from the simulation results.

## Acceleration Requirements and Constraints

In this section we discuss the requirements and resulting constraints on RLA development for  $\mu$  acceleration. In the baseline high-energy collider scenario, the muons must be accelerated from  $\sim 1$  GeV energies at the end of the  $\mu$  production and cooling system, where we expect a beam with an rms bunch length of  $\sim 0.3$  m and  $\sim 1\%$  energy spread, to 2 TeV collision energies. The bunch length must be reduced to  $\sim 3$  mm, to accommodate the focussing at the collision point ( $\beta^* \sim 3$  mm), and the energy spread at collision should be  $\delta E/E \approx 0.001$ . This acceleration must occur with minimal beam loss and emittance dilution.

### Beam lifetime considerations

We can accept only a limited amount of beam loss through decay. The muons decay with a mean lifetime (in the  $\mu$  rest frame) of  $\tau_\mu = 2.2 \mu\text{s}$ , and the muons must accelerate within that lifetime. In the lab frame the lifetime is increased by the relativistic factor  $\gamma = E_\mu/m_\mu$ , where  $E_\mu$  is the  $\mu$  energy and  $m_\mu$  is the mass ( $m_\mu = 0.10566$  GeV). The muon decay rate along the beam path length  $s$  is:

$$\frac{dN}{ds} = -\frac{1}{L_\mu \gamma} N, \quad \text{where } L_\mu = c \tau_\mu \approx 660 \text{ m}, \quad (1)$$

and where we have used the relativistic approximation  $v/c \approx 1$ . In an accelerating section,  $\gamma$  is not constant:

$$\gamma = \gamma_0 + \gamma' s = \gamma_0 + \frac{e V_{rf}}{m_\mu c^2} s,$$

where  $e V_{rf}'$  is the mean accelerating gradient. Using this in the decay equation obtains the solution, within an accelerating section:

$$N(s) = N_0 \left( \frac{\gamma_0}{\gamma_0 + \gamma' s} \right)^{\frac{1}{L_\mu \gamma'}} \quad \text{or} \quad \frac{N(s)}{N_0} = \left( \frac{E_0}{E_{final}} \right)^{\frac{1}{L_\mu \gamma'}} \quad (2)$$

For low losses the exponential factor must be small, which implies:  $L_\mu \gamma' \gg 1$ , or

$$L_\mu \frac{e V_{rf}'}{m_\mu c^2} \gg 1$$

or  $e V_{rf}' \gg 0.16 \text{ MeV/m}$ . For a multiturn  $\mu$  accelerator, this gradient criterion can be rewritten as:

$$E' \rightarrow \frac{E_{final}}{N_{turns} 2\pi R} \gg 0.16 \text{ MeV} / \text{m}.$$

$R$  can be written in terms of the mean bending field  $B$  and the magnetic rigidity  $B\rho$  ( $R = B\rho/B \approx 0.00334 E_{final}(\text{MeV})/B$ ), and  $N_{turns}$  is the total number of acceleration turns. Inserting this into the previous equation obtains the criterion for any multi-turn  $\mu$ -accelerator:

$$\frac{N_{turns}}{B(T)} \ll 300.$$

$B$  refers to the average bending field in the highest energy turn (including straight sections, rf sections, and other non-bending elements in that average). In an RLA, where gradients can be greater than 10 MV/m, mean bending fields can be several T, and the total number of turns are  $< 20$ , this criterion is readily met.

### General Phase Space Considerations

The collision requirements set the longitudinal phase-space area of the beam at collisions to  $\sim 3\text{mm} \times 2 \text{ GeV}$  ( $\Delta E/E = 0.001$  for 2 TeV), or 0.02 eV-s. This invariant area is not much larger than the beam emittance at the beginning of acceleration. Only a limited degree of emittance dilution in the accelerator could be acceptable.

The longitudinal invariant area is in  $\Delta E - \Delta s/c$ , where  $\Delta E$  is the beam energy width,  $\Delta s$  is the bunch length, and  $c$  is the speed of light. From previous lattice studies, we expect that transport acceptances will be limited in  $\Delta E/E$  to a few per cent. Thus as  $E$  increases,  $\Delta E$  can also be allowed to increase, and this permits a reduction in  $\Delta s$ .

The rf wavelength also constrains the bunch-length; the bunchlength must be less than the rf wavelength. Also, for efficient acceleration, the beam should be placed entirely at or near "crest", or  $\phi \sim 0^\circ$ , where acceleration is maximum. The bunch should be as short as practical

to minimize acceleration variations and therefore energy width. At  $\mu$ -accelerator parameters, we actually want a beam with full phase width  $\Delta\phi < \pm 30^\circ$  or  $\sigma < \sim 15^\circ$ . (This guideline is more strictly defined below.) We expect that accelerator rf system costs will decrease with decreasing rf wavelength; under this constraint we would like to reduce the rf wavelength where the bunch-length compression allows it. Thus when adiabatic damping (of  $\Delta E/E$ ) permits bunch-length compression, we would compress the bunch and transfer the beam to a higher-frequency (shorter wavelength) RLA for further acceleration.

The relatively large changes in energy and in bunch-length lead naturally to consideration of a sequence of RLAs, with the rf wavelength decreasing with increasing RLA energy while the bunch length decreases. Following earlier accelerator studies, it is natural to increase energies by a factor of  $\sim 10$  in each RLA, while simultaneously increasing rf frequency. From these guidelines, we initiated the simplified 3-RLA scenario with the parameters displayed in Table 2. In this scenario we accelerate from 2 to 2000 GeV using three 10-pass RLA's, with bunch-length reduction to 3mm. This scenario is discussed in greater detail below.

The same RLA system could be used to accelerate both  $\mu^+$  and  $\mu^-$  bunches. The oppositely charged bunches would propagate around the RLAs in opposite directions. If the bunches are injected into opposite sides of each RLA at the beginning of the separate linacs, then energy match of the beams in each arc is obtained, as well as phase matching across the arcs. Separate (but symmetric) transport lines transferring the beams between RLA's and into the collider would be needed.

### Phase-space matching for stable acceleration

To minimize phase-space mismatch and consequent dilution, it is desirable to minimize bunch shape oscillations by matching the bunch in both energy and phase spread to the stability region or "rf bucket" associated with the longitudinal motion parameters. Figure 2 shows the characteristic longitudinal stability separatrix. The stability region extends in phase from  $-\phi_s$  past the synchronous phase  $\phi_s$  to the solution  $\phi_2$  of:

$$\phi_2 \cos \phi_s - \sin \phi_2 = \sin \phi_s - \phi_s \cos \phi_s.$$

To reasonable accuracy,  $\phi_2 \cong 2\phi_s$ . The extreme energy acceptances  $\pm \Delta E/E$  are given by:

$$\frac{\Delta E}{E} = \pm \sqrt{\frac{eV_{rf}\lambda}{EM_{56}}} \sqrt{\frac{2(\sin \phi_s - \phi_s \cos \phi_s)}{\pi}} \cong \pm \sqrt{\frac{2eV_{rf}\lambda}{3\pi EM_{56}}} \phi_s^3, \quad (3)$$

where  $V_{rf}$ ,  $\lambda$  are the rf voltage (per linac) and wavelength.  $M_{56}$  is the chromaticity of an arc:  $M_{56} = dz/d(\Delta E/E)$ , where  $z = \lambda\phi/(2\pi)$ . (In a synchrotron,  $M_{56} = \lambda h/\gamma^2$  for a full turn.)  $M_{56}$  can be calculated by integrating the dispersion  $\eta$  around the arc:

$$M_{56} = \int \eta d\theta.$$

The separatrix is correct for continuous motion in a synchrotron. The small number of turns in an RLA makes the synchrotron motion approximation somewhat inaccurate, but it is a useful guideline for RLA design.

However, the stepped process of acceleration and compression provides distortion, particularly with the relatively large steps in an RLA. This distortion must be limited in order to minimize phase-space dilution by filamentation and to avoid beam loss due to beam exiting the stable acceleration region. In particular, particle motions within any single acceleration step must remain within the stable region. Since the energy spread must remain within the bucket, the energy spread within each acceleration step must be less than the rf bucket width. In any single step, particle energy gains vary from maximum ( $eV_{rf}$ ) to that at the edge of the separatrix ( $-eV_{rf}\cos(2\phi_s) \equiv eV_{rf} - 2eV_{rf}\phi_s^2$ ). We require that the width in energy gain be less than the full beam-energy width:

$$2eV_{rf}\phi_s^2 \leq 4\sigma_E .$$

This limits  $\phi_s$  to relatively small values; for the RLA's in the scenario in Table 1 it implies that  $\phi_s < \sim 23^\circ, 16^\circ, 12^\circ$  for RLAs 1, 2, and 3 respectively. With matched acceleration, the rms bunch length is  $\sim \phi_s/2$ . Therefore these limits imply physical bunchlength limits of  $\sigma_z < 10\text{cm}, 1.5\text{cm},$  and  $0.3\text{cm}$ , for RLAs 1, 2, 3 (100, 400, and 1600 MHz). These are close to the minimum in each case, which means that we can permit little bunching within the body of each RLA.

In initial scenarios, we have therefore chosen to keep the bunch length approximately constant within the RLA's. Maintaining a constant phase-space-area bucket then demands that the energy width of the stable acceleration region must remain constant. From Equation (3), maintaining a matched energy spread for fixed bunch length requires  $\Delta E/E$  to decrease as  $1/E$ , which therefore implies that  $M_{56}$  must increase linearly with energy  $E$ . That condition was used in our initial simulations to set  $M_{56}$  from turn to turn. This phase-space matching minimizes bunch lengths within the RLAs, which in turn reduces amplitude-dependent nonlinearities and also reduces the amplitude of bunch length oscillations, both of which can cause phase-space dilution. A similar matching condition on  $M_{56}$  occurs naturally in microtron design.

### Bunch compression

However we can bunch the beam in the transport between RLA's, using a buncher rf system followed by a compression arc. In the buncher the beam passes at zero crossing ( $\phi_s = -90^\circ$ ), so that the center of the beam is not accelerated. The rf puts a position-dependent energy correlation on the beam:  $\Delta E = eV_{rf} \sin(\phi) \equiv eV_{rf} \phi$ . The rf voltage and frequency are chosen so that the bunch length is  $\Delta\phi < \pm 60^\circ$ , and the rf voltage times the phase spread is equal to the desired energy spread ( $eV_{rf} \Delta\phi_{\text{total}} \equiv \Delta E_{\text{total}}$ ). The rf buncher is followed by a transport into the arc, and the chromaticity of that transport is chosen to provide bunching into the linac. The condition for maximal bunching is:

$$\frac{2\pi M_{56} eV_{rf}}{\lambda E_\mu} = 1 ,$$

The larger phase spread permitted for bunching implies that a higher frequency could be used for the bunchers. For example, following an RLA with phase acceptances of  $\pm 15^\circ$ , a zero-crossing buncher in which these phases are frequency-multiplied, up to  $\pm 60^\circ$ , could be used,

and this is obtained by using an rf frequency of up to 4 times the RLA rf. Since for bunching we require gradient rather than peak voltage, this reduces the rf voltage requirements proportionately. This increase of frequency for bunching is used in the present scenarios.

### Scenario descriptions

Based on these considerations we have developed the scenario described in Table 2. This is a modularized 3-RLA case. In each stage the energy is increased by a factor of 10 (2 to 20 to 200 to 2000 GeV). The rf frequency is also changed by a factor of 4 from RLA to RLA, from 100 to 400 to 1600 MHz. Each RLA consists of two linacs (1 to 10 to 100 GeV) with recirculating arcs connecting them, and a total of ~10 turns in each stage. A three-RLA accelerator is displayed in Figure 3.

Before entering the first RLA, and between subsequent RLA's, bunchers (1, 2, and 3) consisting of an rf system plus a compressor arc are inserted. The buncher rf frequencies are matched to the reduced bunch-length rf of the subsequent RLA. All of the bunchers are at zero-crossing rf phases, and at frequencies of 100, 400, and 1600 MHz before RLA's 1, 2, and 3 respectively.  $V_{rf}$  and  $M_{56}$  are set by phase space matching into the accelerating buckets of each linac, and their values are displayed in Table 2. In this initial scenario the RLA linacs are set at fixed accelerating phases. Therefore, this scenario is "separated function" in that bunch-length reduction is primarily accomplished by the bunchers, while the RLA's are used for acceleration. The total  $V_{rf}$  required for the bunchers is 7.45 GV, ~3% of that used in acceleration.

The rf frequencies approximate those of existing or expected rf systems. In particular the high-frequency rf is similar to the TESLA parameters (1300 MHz), which is designed under high-gradient, low-cost considerations comparable to our requirements. Both the rf frequency jump factor of 4 and the number of passes (10) are arbitrarily set to initiate scenario studies; however we do expect an eventual optimum to be similar.

Another scenario, presented by Palmer in July 1995,<sup>5</sup> is displayed in table 3, and demonstrates some of the possible variations in design. In that scenario, beam is accelerated from 1 GeV to 2 TeV using 4 RLA steps with top energies of 8, 75, 250 and 2000 GeV. The 250 GeV step is a suitable accelerator for a 250×250 GeV collider. Buncher transitions between RLAs are included. Similar performance to the 3-RLA scenario is obtained, but with slightly larger losses and dilution due to the additional RLA. Simulation studies of this scenario are also reported below.

### Simulations and analyses

We have developed the 1-D program  $\mu$ RLA to simulate the RLA longitudinal motion. In that program particle energy and position offsets are calculated from turn to turn. On each passage through a linac, particle energies change following:

$$\Delta E \rightarrow \Delta E + eV_{rf} (\cos \phi - \cos \phi_s) ,$$

while the synchronous energy increases by  $eV_{rf} \cos \phi_s$ . On each pass through an arc, particle phases change by:

$$\phi \rightarrow \phi + M_{56} \frac{2\pi}{\lambda} \frac{\Delta E}{E} + M_{566} \frac{2\pi}{\lambda} \left( \frac{\Delta E}{E} \right)^2 + \dots$$

where we have included first and second order chromaticities  $M_{56}$  and  $M_{566}$ . Note that  $\phi$ ,  $M_{56}$ , and  $M_{566}$  can be changed from turn to turn.

As a simplified first example, which we use as a proof of principle, we consider in detail the 3-RLA scenario with the parameters of Table 2. We have simulated this scenario using  $\mu$ RLA, and some results are summarized in Table 4, and are displayed in figure 4. Some phase-space dilution and mismatch does occur, particularly in transfers between RLAs. However the rms emittance dilution is  $< \sim 5\%$  per RLA or 15% over the entire system. Particle loss through the beam dynamics is less than 1%. Particle loss through  $\mu$ -decay is somewhat larger, but is less than  $\sim 5\%$  per RLA or  $\sim 12\%$  over the entire system. Bunch compression to  $\sigma < 0.003$  m is obtained through rebunching and matching with the frequency increase from RLA to RLA, and is acceptable.

The 4-RLA scenario has also been simulated using  $\mu$ RLA, and results are summarized in Table 5 and displayed in figure 5. The rms emittance dilution is also  $\sim 5\%$  per RLA, or  $\sim 20\%$  over the full system. Particle loss through the beam dynamics is  $< 1.5\%$ . Particle loss through  $\mu$ -decay is somewhat larger, but is less than  $\sim 20\%$  over the entire system. Thus the beam dynamics is a bit worse than the 3-RLA, mostly due to the additional RLA and the resulting additional mismatch. The greatest mismatch and emittance growth occurs in the transition and matching to the third RLA at 75 GeV, since the frequency change to higher frequencies occurs at relatively low energies. However, even this mismatch is acceptable, and it could be reduced by further optimization.

These simulations demonstrate that a cascade of RLAs can provide acceptable acceleration with bunching for a  $\mu^+\mu^-$  collider, with minimal dynamic and decay beam loss and emittance dilution. The scenarios are certainly unoptimized, and do not exploit the full degree of freedom possible in the multiple RLA scenario. The results do set a baseline for the exploration of other scenarios.

## Decay losses

We have also calculated the amount of beam loss through decay in these scenarios. For this purpose we must set mean accelerating gradients for the linacs and mean bending fields for the arcs of the RLA's to determine their lengths. Once these are estimated, equations 1 and 2 can be evaluated for each section of the RLA's, obtaining beam survival rates. In the 3-RLA scenario we use gradients of 13, 18, and 18 MV/m for RLA's 1, 2, and 3 respectively, and mean bending fields of 3.3, 4.45, and 5.6 T for their arcs. At these parameters 87.4% of the initial muons survive the complete acceleration process. In the 4-RLA scenario, we use gradients of 5.5, 11, 16.2, and 19.4 MV/m for linacs 1, 2, 3, 4 and 3.4, 4.2, 5.2 and 5.6 T arc bending fields. At these parameters 81.4% of the muons survive through acceleration. In this second case overall decay is a bit larger because of the additional RLA and the larger number of turns, but not greatly larger. These cases show that multiple-RLA acceleration of muons is sufficiently fast to avoid decay, and, over a broad range in design variation,  $\mu$ -survival of  $\geq 80\%$  can be readily obtained.



## Wakefield Considerations

The initial studies included only single-particle dynamics. However a high-luminosity  $\mu^+\mu^-$  collider will have very high-density bunches, with  $\sim 10^{12}$  or more particles per bunch. At these high-intensities, collective effects can be important. In the short bunches prepared for the collider, the dominant effect is expected to be the short-range wake field. Mosnier and Napoly<sup>6</sup> have evaluated wakefields in the TESLA 9-cell structure (1300 Mhz,  $\sim 1$ m length), which is designed to accelerate at 25 MV/m and is thus very similar to the rf system we would need for the high-energy high-frequency RLA(s). They obtain a maximum wakefield across an electron bunch of 1mm length of  $\sim 15$  V/pC. For  $10^{12} \mu$  ( $1.6 \times 10^5$  pC), this is 2.4 MV or almost 10% of the accelerating voltage. Our bunches are  $\sim 4$  times longer than 1mm, and the short-range wakefield is reduced in proportion to the square root of that length, so the wakefield would be a factor of 2 smaller. It is also proportional to  $\sim 1/a^2$ , where  $a$  is the cavity aperture. This aperture could be changed, and it is naturally larger for longer wavelength (lower frequency) rf. Other cavity shape and high-order mode coupler changes could also change the wake-fields, although the TESLA design should be a relatively low wake-field design. We may also want more than  $10^{12} \mu$ 's per bunch for high luminosity, and scenarios with up to  $4 \times 10^{12}$  have been generated.

For our recirculating linac scenarios, we expect that the largest wake-field effects will occur in the highest-energy (2 TeV) recirculating linac, since that linac has the highest frequency rf and the shortest bunches. We have studied these effects by simulations of particle motion which include wake-fields in the final 200 to 2000 GeV linac of the 3RLA scenario. To include wakefield nonlinearity effects in our simulations, we have used a simplified short-range model in which the longitudinal wakefield deceleration on each particle is proportional to the charge in front of the particle, with the full bunch charge giving the total wakefield. (This model was used in the CEBAF FEL design.<sup>7</sup>) Following the TESLA values (scaled to 4mm bunch length) we estimate a total wakefield of  $\sim 7.5$  V/pC, or 1.2—4.8 MV wakefield per 25 MV acceleration for  $1\text{--}4 \times 10^{12} \mu$ 's.

The first-order and second-order wakefield effects (magnitude and slope) can be compensated by increasing the rf voltage and changing the accelerating phase. Higher order effects are not compensated, and can give nonlinear distortion to the motion, causing emittance dilution and eventual beam loss. Some simulation results are displayed in table 6 and in figure 6. For 1.0 and 2.5 MV (per 25 MV) cases we can increase the rf voltage (by  $\sim 4\%$  and  $12.4\%$ , respectively) and shift the rf phases from  $12^\circ$  to  $18^\circ$  and  $25^\circ$ , respectively. We then obtain similar performance to the zero wakefield case, with similar distortion and phase space dilution. For 5 MV, the rf voltage would need to be increased by  $\sim 30\%$  and the rf phase  $\phi_s$  moved to  $35^\circ$ . Significant orbit distortion is seen (emittance dilution of  $\sim 30\%$ ). Although no beam loss occurs, the phase space distortion is at the limit of acceptability.

Thus for moderate size bunches ( $1\text{--}2 \times 10^{12}$ ) the wake-fields can be compensated, but much larger charges could lead to significant distortion and beam loss. These intensities are somewhat uncomfortably close to the intensities at which wake-field effects can become a limitation. Significant monitoring and more accurate evaluations of wake-fields are needed; it is important to ensure that wake-fields are minimized.

## DISCUSSION ON DESIGN AND OPTIMIZATION

While we have studied the longitudinal motion in acceleration in RLA systems, we have not yet developed a complete design, which would include beam transport design details, as well as more explicit linac specifications, and injection/extraction.

For injection, we have used idealized  $\sim 1$ -GeV beams with an energy spread and bunch length within reasonable reach of ionization cooling systems. However we do not yet have a complete cooling system, and we will need some sort of initial acceleration and matching system to take the beam from the low-energy of final cooling into the RLA system. This will probably be some sort of initial  $\sim 1$  GeV low-frequency linac, with some sort of initial bunching. Beam production and cooling studies should more precisely define the  $\mu$ -source, which in turn will specify the injector linac, and the revised matching conditions may affect the initial portions of the RLA system.

We have not exploited the full range of flexibility inherent in the multiple RLA design. The number, rf frequencies, and acceleration energies of the RLA's could be changed. The synchronous phase  $\phi_s$  can be changed from pass to pass. Also the chronicity,  $M_{56}$ , can be changed on each turn, and different optimization paths can be considered. Higher order chronicity control ( $M_{566}$ ) with sextupoles is also possible, and one can consider adding higher-harmonic rf, which could improve bunching within an RLA. These options should be more fully developed in future studies.

In the present scenarios, we have separated most of the bunch-length compression into the transfers between RLA's, with the RLA's used for phase-space matched acceleration. This was partially due to the physics constraints, but was also due to the conceptual simplification in separating these functions. Scenarios which transfer more of the bunch-length compression into the body of the RLA's should be developed. These scenarios could reduce the relatively large energy apertures required in the initial RLA passes. As noted above, including higher-harmonic rf would facilitate this.

In a multiturn RLA system there is a balance between rf acceleration and beam transport cost/requirements. Increasing the number of turns per RLA directly reduces the linac lengths and therefore linac costs, but it also increases the beam transport cost and complexity. We do not yet have cost estimates that are adequate to obtain an accurate optimum, but we have identified some of the key issues and requirements. In the following sections some of these factors to be considered in developing an optimum design are discussed.

### rf Considerations

We need a separate rf linac system for each RLA, with lower frequencies for the initial lower-energy RLAs, where the beam has a relatively long bunch length, and higher frequencies for the high energy end, where the bunches are shortened, since higher-frequencies are expected to be less expensive. However, higher-frequency rf cavities have larger wake-fields, and do require low-temperature cryogenics with present technology. Very high-gradient is not essential in the acceleration, but minimal cost is. The 3-RLA scenario requires  $\sim 200$  GV of rf acceleration, while the 4-RLA scenario requires  $\sim 100$  GV; these are both quite large and would require  $\sim 5$ — $10$  km at  $20$  MV/m. This gradient must also be larger than the longitudinal wake-field by an order of magnitude. Comparisons with calculated TESLA wake-fields indicate that

we may be close to this limit in the high-energy RLA for our highest-intensity ( $N_\mu > 2 \times 10^{12}$ ) cases. Modifications which can improve this ratio (i. e., higher gradient or smaller wake-fields) are desirable.

### Transport considerations

The beam transports for the recirculation arcs are relatively straightforward, but are nontrivial, since they require good transverse matching throughout the system to avoid emittance dilution. Each transport must be achromatic (matched to zero dispersion), and also must have a chromaticity  $M_{56}$  matched to the bunching requirements. A transport modeled on the CEBAF RLA could be used.<sup>8</sup> High field is not required, and even conventional fields ( $B < 2T$ ) are adequate.

The  $M_{56}$  values are small compared to the natural chromaticities. The average dispersion in an arc (given by  $\eta = M_{56}/\pi$ ) varies from  $\sim 0.1$  to  $1$  m in these cases. Flexible momentum compaction lattices, where the average  $\eta$  is reduced by including perturbations to negative  $\eta$ , are indicated for some of these arcs.<sup>9</sup>

A significant concern is the relatively large energy spreads (up to 5% rms) which occur in the initial turns of the lower energy RLA's. Detailed design of arc transports which can accommodate these, without losses or emittance dilution, will be a challenge. It is likely that the scenarios should be modified to reduce the energy spread requirements, possibly by keeping the bunches longer, which may require lower-frequency or multi-harmonic rf systems. We note that the 4-RLA example has relatively large energy-spread requirements, and that is due to the use of high-frequency rf at relatively low energies.

Since the beam passes through a different return arc on each turn, the total amount of beam transport is relatively large ( $\sim 85$ km of arcs in the 3-RLA scenario, and  $160$ km for the 4-RLA case.). The transport can easily become **very** expensive, so cost-saving designs are needed, such as multiple-aperture<sup>10</sup> or rapid-cycling hybrid designs.

## SUMMARY

We have demonstrated the general principle of muon acceleration with bunch compression in a multiple recirculating linac scenario. The longitudinal simulations show that acceleration with minimal beam loss from decay ( $< 20\%$ ), and with minimal longitudinal phase space dilution is possible. Wake-field effects can be compensated, although wake-field limitations are uncomfortably close to high-luminosity peak bunch intensities. More complete designs, with beam transport and rf layouts and specifications, should next be developed.

### Acknowledgments

We acknowledge important contributions from our colleagues, especially F. Mills, S. Simrock, R. Noble, J. Norem, and R. Palmer.

## References

1. Proceedings of the Mini-Workshop on  $\mu^+\mu^-$  Colliders: Particle Physics and Design, Napa CA, Nucl. Inst. and Meth. A350, 24-56(1994).
2. Proceedings of the 2nd Workshop on Physics Potential & Development of  $\mu^+\mu^-$  Colliders, Sausalito, 1994, to appear as AIP Conf. Proc. (1995).
3. Proceedings of the Workshop on Beam Dynamics and Technology Issues for  $\mu^+\mu^-$  Colliders, Montauk, October 1995, to appear as AIP Conf. Proc. (1996).
4. D. Neuffer, "Acceleration to Collisions for the  $\mu^+\mu^-$  Collider", to appear in ref. 3 (1996).
5. R. Palmer, presented at the 2+2 TeV  $\mu^+\mu^-$  Collider Collaboration meeting, Fermilab, July 1995 (unpublished).
6. A. Mosnier and O. Napoly, Proc. XV Int. Conf. on High Energy Accelerators, J. Rossbach, ed., p. 963 (1992)
7. Laser Processing Consortium, Free Electron Lasers for Industry Volume 2: UV Demo Conceptual Design, CEBAF, May 1995.
8. CEBAF Design Report, CEBAF, Newport News VA (1986) (unpublished).
9. S. Y. Lee, K. Y. Ng, and D. Trbojevic, Physical Review E 48, p. 3040 (1993).
10. S. Kahn, G. Morgan, and E. Willen, "Recirculating arc dipole for the 2+2 TeV  $\mu^+\mu^-$  Collider", Montauk, ref. 3, October, 1995.

**Table 1: Parameter list for a 4 TeV  $\mu^+\mu^-$  Collider**

<u>Parameter</u>	<u>Symbol</u>	<u>Value</u>
Energy per beam	$E_\mu$	2 TeV
Luminosity	$L=f_0 n_s n_b N_\mu^2 / 4\pi\sigma^2$	$10^{35} \text{ cm}^{-2}\text{s}^{-1}$
<b>Source Parameters</b>		
Proton energy	$E_p$	30 GeV
Protons/pulse	$N_p$	$2 \times 3 \times 10^{13}$
Pulse rate	$f_0$	15 Hz
$\mu$ -production acceptance	$\mu/p$	.2
$\mu$ -survival allowance	$N_\mu/N_{\text{source}}$	.33
<b>Collider Parameters</b>		
Number of $\mu$ /bunch	$N_{\mu\pm}$	$2 \times 10^{12}$
Number of bunches	$n_B$	1
Storage turns	$n_s$	1000
Normalized emittance	$\epsilon_N$	$3 \times 10^{-5} \text{ m-rad}$
$\mu$ -beam emittance	$\epsilon_t = \epsilon_N / \gamma$	$1.5 \times 10^{-9} \text{ m-rad}$
Interaction focus	$\beta_0$	0.3 cm
Beam size at interaction	$\sigma = (\epsilon_t \beta_0)^{1/2}$	2.1 $\mu\text{m}$

**Table 2: Parameters for an idealized 3-RLA acceleration scenario**  
(The Bi are bunchers; RLAI are multipass recirculating linacs)

Cycle	Energy (GeV)	rf frequency	passes	Bunch length $\sigma$	$\delta E/E$	$V_{rf}$ per linac pass	$\phi_{\mu}$	$M_{se}$ per arc	decay loss	Time ( $\mu s$ )
B1	2	100 MHz		25 $\rightarrow$ 7	1 $\rightarrow$ 4%	0.2GV	90°	5.0m		
RLA 1	2 $\rightarrow$ 20	100 MHz	9	7 cm	4 $\rightarrow$ 0.4 %	1	15°	0.4 $\rightarrow$ 2.8	6.1%	8
B2	20	400 MHz		7 $\rightarrow$ 1.5	0.4 $\rightarrow$ 2%	1.25	90°	2.0		
RLA 2	20 $\rightarrow$ 200	400 MHz	10	1.5 cm	2 $\rightarrow$ 0.2%	10	13°	0.25 $\rightarrow$ 1.75	3.7%	65
B3	200	1.6 GHz		1.5 $\rightarrow$ 0.3	0.2 $\rightarrow$ 1.0%	6	90°	1.2		
RLA 3	200 $\rightarrow$ 2000	1.6 GHz	10	0.3 cm	1.0 $\rightarrow$ 0.1%	100	12°	0.3 $\rightarrow$ 2.1	3.4%	585

**Table 3: Parameters for a 4-RLA acceleration scenario**

Cycle	Energy (GeV)	rf frequency	passes	Bunch length $\sigma$	$\delta E/E$	$V_{rf}$ per linac pass	$\phi_{\mu}$	$M_{se}$ per arc	decay loss	Time ( $\mu s$ )
B1	1	100 MHz		25 $\rightarrow$ 7.5	1.5 $\rightarrow$ 5%	0.08GV	90°	6.0m		
RLA 1	1 $\rightarrow$ 9.6	100 MHz	8	7.5 $\rightarrow$ 5.0	5.0 $\rightarrow$ 1 %	0.5	20°	0.4 $\rightarrow$ 2.1	7.5%	5.6
B2	9.6	400 MHz		5 $\rightarrow$ 1.6	1 $\rightarrow$ 4.5%	0.86	90°	1.1		
RLA 2	9.6 $\rightarrow$ 79	400 MHz	12	1.6cm	4.5 $\rightarrow$ 0.5%	3	15°	0.1 $\rightarrow$ 1 m	5.3%	40
B3	79	1.3 GHz		1.6 $\rightarrow$ 0.5	0.5 $\rightarrow$ 1.5%	2.64	90°	1.0		
RLA 3	79 $\rightarrow$ 250	1.3 GHz	18	0.5	1.5 $\rightarrow$ 0.5%	5	16°	0.1 $\rightarrow$ 0.4	3.1%	96
B4	250	2.0 GHz		0.5 $\rightarrow$ 0.3	0.5 $\rightarrow$ 0.8%	8.6	90°	1.8		
RLA 4	250 $\rightarrow$ 2000	2.0 GHz	18	0.3cm	0.8 $\rightarrow$ 0.1%	250	15°	0.2 $\rightarrow$ 1.5	4.1%	662

**Table 4:  $\mu$ RLA Simulation Results for the 3-RLA scenario**

Cycle	Energy (GeV)	rf frequency	Bunch length(°)	$\delta E_{rms}$ (GeV)	emittance (eV-ms)
B1	2.1	100 MHz	5.8	0.08	13.1
RLA 1	19.5	100 MHz	5.9	0.08	13.4
B2	19.5	400 MHz	4.1	0.48	13.6
RLA 2	204.6	400 MHz	4.8	0.45	14.0
B3	204.6	1.6 GHz	4.6	1.80	13.8
RLA 3	2063	1.6 GHz	4.6	2.13	14.6

**Table 5:  $\mu$ RLA Simulation Results for the 4-RLA scenario**

Cycle	Energy (GeV)	rf frequency	Bunch Length	$\delta E_{rms}$ (GeV)	Emittance (eV-ms)
B1	1.1	100 MHz	8.9°	0.05	12.2
RLA 1	9.6	100 MHz	5.6°	0.08	12.6
B2	9.6	400 MHz	5.8°	0.33	12.9
RLA 2	79.2	400 MHz	6.4°	0.31	12.7
B3	79.2	1.3 GHz	7.4°	0.87	13.4
RLA 3	252.4	1.3 GHz	7.4°	0.95	14.5
B4	252.4	2.0 GHz	6.5°	1.67	14.6
RLA 4	1993	2.0 GHz	6.1°	1.89	14.9

**Table 6:  $\mu$ RLA Simulation Results with wakefields for a 2 TeV recirculating linac.** In these simulations we used initially Gaussian beams with 20 eV-ms normalized rms emittance at 200 GeV.

Case	Wakefield Amplitude	Accelerating phase	rf voltage depression	Bunch Length	$\delta E_{rms}$ (GeV)	Final Emittance
1	0	13°	0%	5.58°	2.41	22.5 eV-ms
2	1 MV/m	18°	4.5%	4.89°	2.68	22.0
3	2.5	25	12%	6.06°	2.17	21.6
4	5	35	26%	6.66°	2.71	31.3



## Recirculating Linac

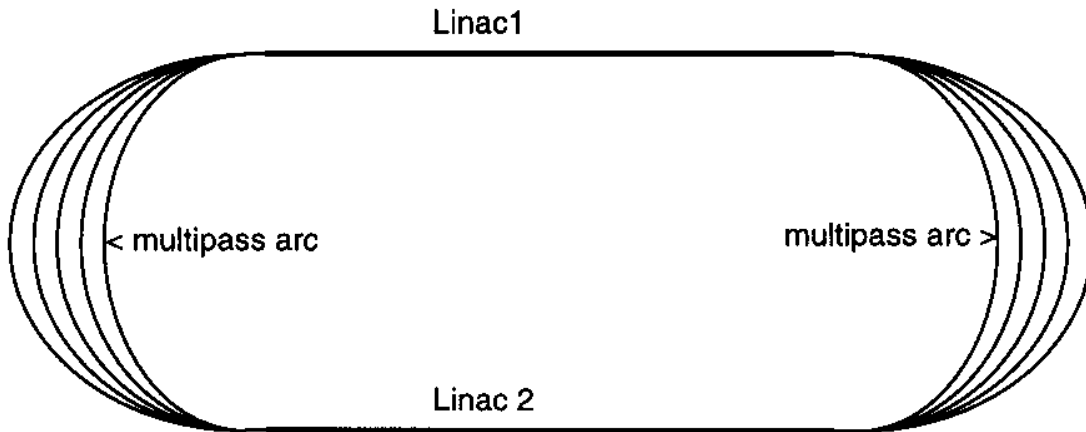


**Figure 1.** Schematic view of a recirculating linac (RLA). In the RLA, the beam is accelerated through several passes of the linacs. On each return arc, the beam passes through a different transport path, matched to the increasing beam energy. Magnetic fields are fixed, and the number of return transports (per arc) equals the number of linac passes.

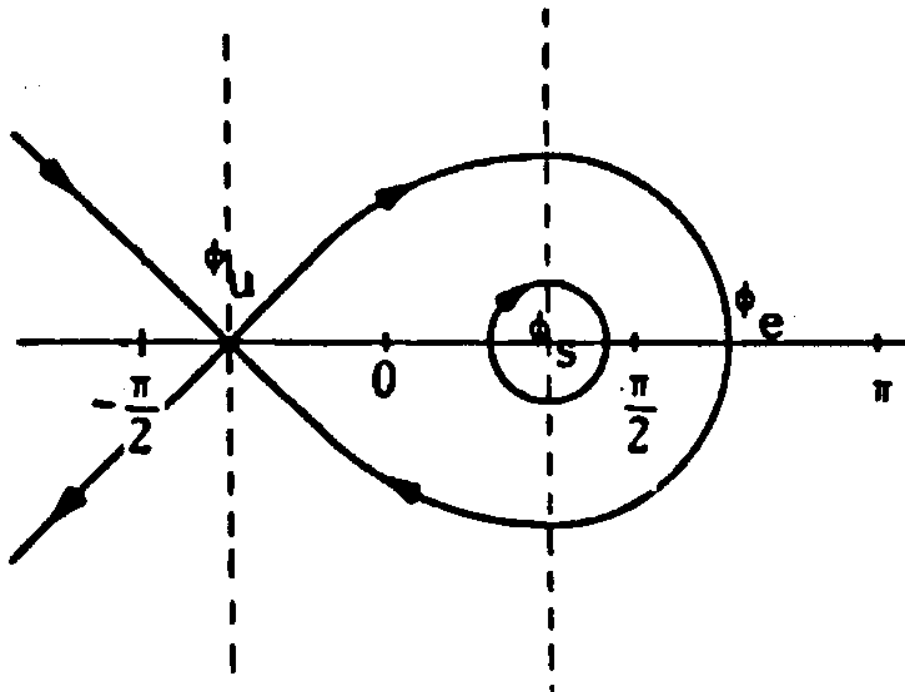


**Figure 2.** Schematic view of a stable accelerating bucket, showing stable phase and energy spread widths. The stable bucket extends (horizontally) in phase from  $\phi_u = -\phi_s$  past  $\phi_s$  to  $\phi_e \equiv 2\phi_s$ . The vertical scale is energy width, with the width in  $\Delta E/E$  at  $\phi_s$  given by equation 3.



### $\mu^+\mu^-$ Accelerator and Collider System

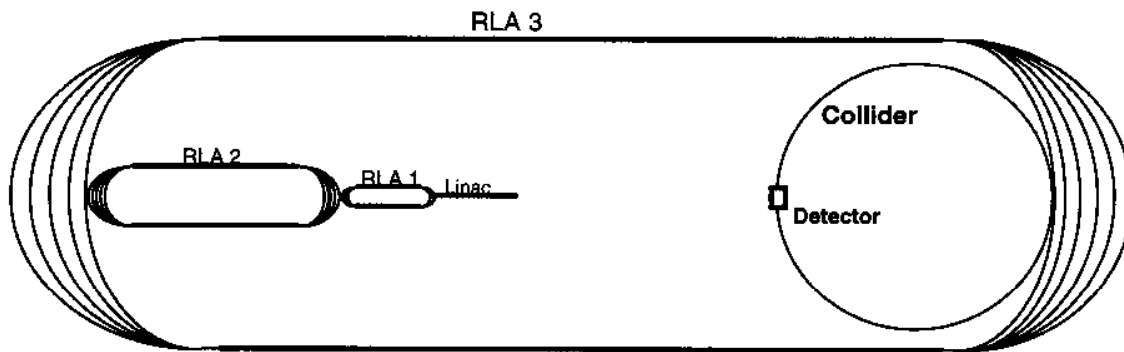


**Figure 3.** Conceptual view of an RLA-based accelerator, showing a linac feeding beams into a sequence of 3 recirculating linacs (RLA1, RLA2, RLA3) followed by a collider ring. Note that the drawing is not to scale (size change from RLA to RLA would be greater), and the separation between lines in the arcs is exaggerated in this sketch. (There will also be more arc beam lines than displayed, and the separations could be vertical.)

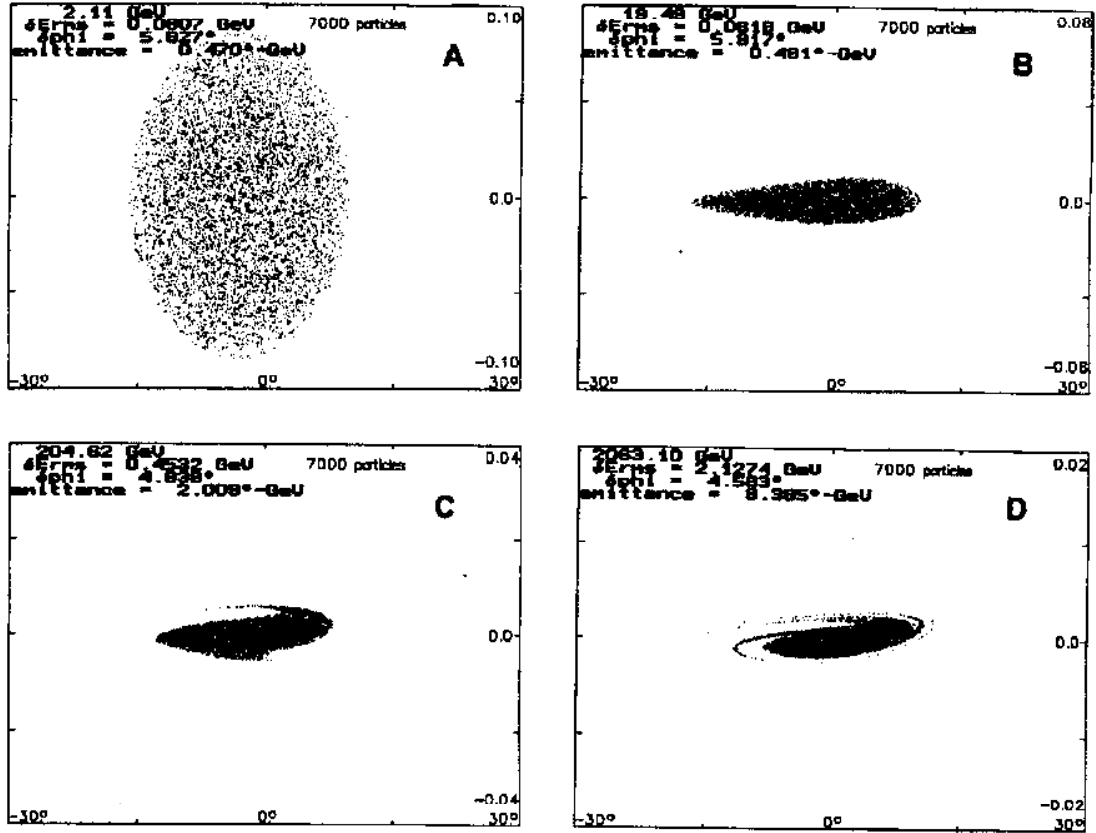


**Figure 4.** Some simulation results from  $\mu$ RLA. In these simulations a beam is accelerated from 2GeV to 2000 GeV through the three cascaded RLAs of table 2, with bunching at the beginning of each linac. An initially bunched beam for RLA 1 is shown in Fig. 4A, and beam phase-space distributions at the end of RLAs 1, 2, and 3 are shown in 4B, 4C, 4D. The vertical and horizontal scales are  $\delta E/E$  and  $\delta\phi$ , respectively. Note that rf frequency increases from 100 to 400 to 1600 MHz from RLA to RLA. The beam is accelerated with very little loss from beam dynamics acceptance and with a longitudinal emittance dilution of  $\sim 12\%$ . Beam loss from decay would be  $\sim 12\%$ .

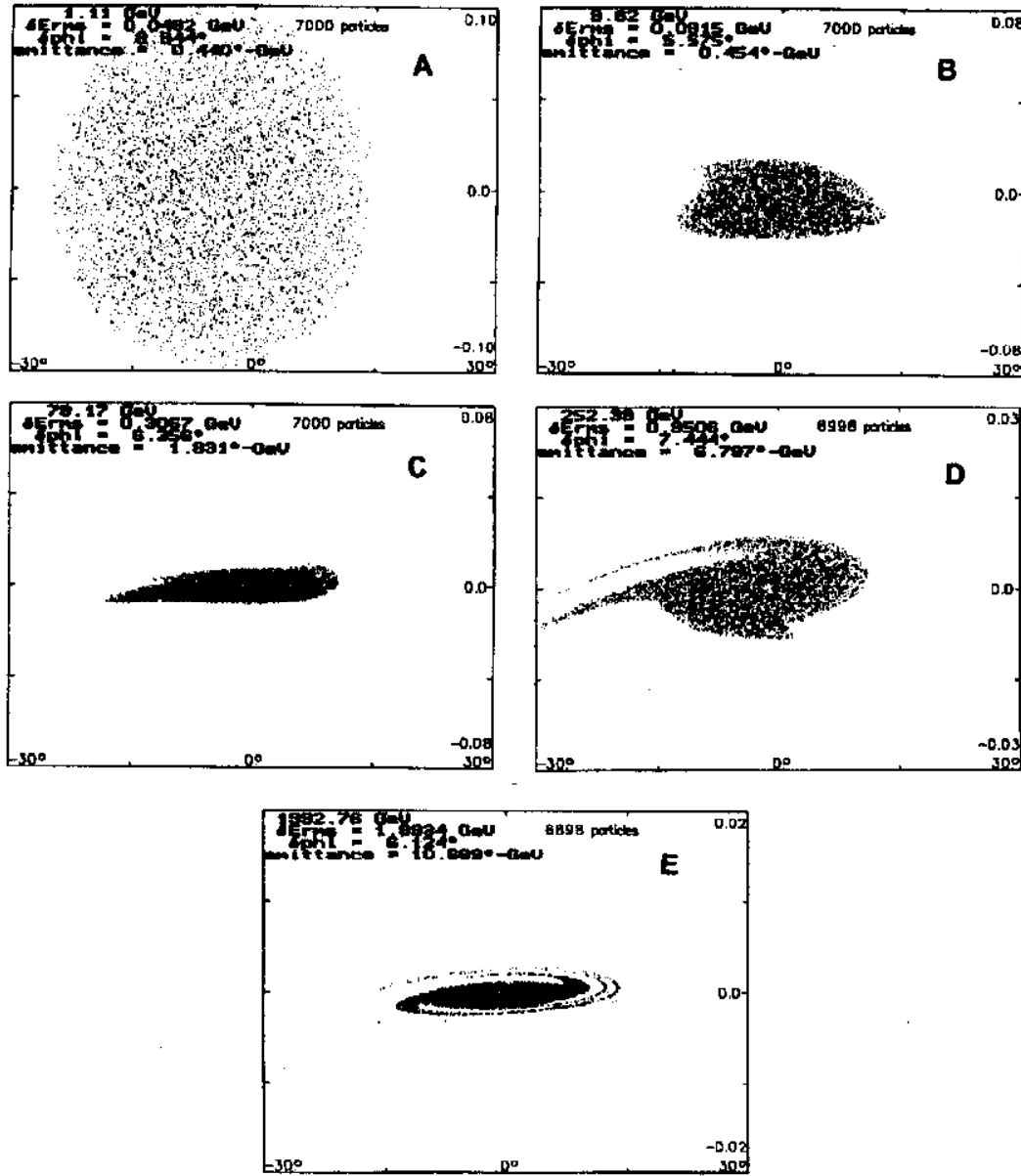


**Figure 5.** Some simulation results from  $\mu$ RLA. In these simulations a beam is accelerated from 1 GeV to 2000 GeV through the four cascaded RLAs of table 3, with bunching at the beginning of each linac. An initially bunched beam for RLA 1 is shown in Fig. 5A, and beam phase-space distributions at the end of RLAs 1, 2, and 3 and 4 are shown in 5B, 5C, 5D, 5E. The vertical and horizontal scales are  $\delta E/E$  and  $\delta\phi$ , respectively. Note that rf frequency increases from 100 to 400 to 1300 to 2000 MHz from RLA to RLA. The beam is accelerated with  $< 1.5\%$  loss from beam dynamics acceptance and with a longitudinal emittance dilution of  $\sim 20\%$ . Beam loss from decay would be  $\sim 20\%$ .

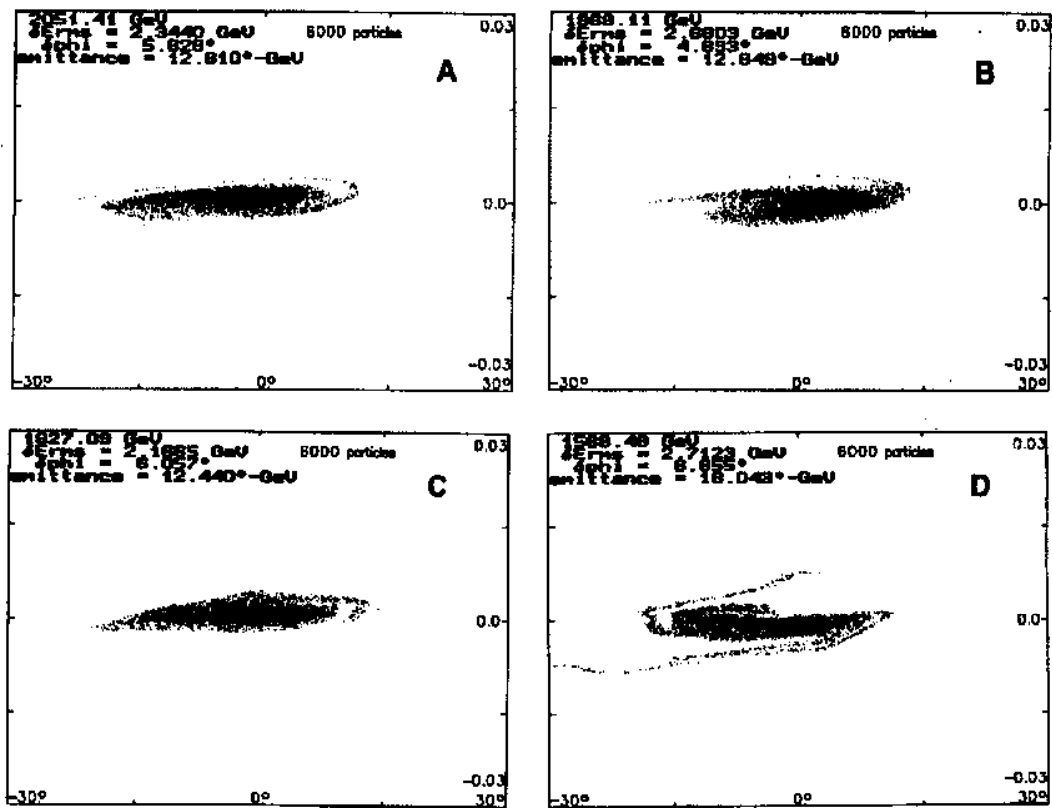


**Figure 6.**  $\mu$ RFA simulation results with wake fields, with beam accelerated from 200 to  $\sim 2000$  GeV in the 10-turn RLA of Table 2. In Figure 6A, B, C, and D we display beam distributions at the end of 10 turn accelerations with wake fields of 0, 1, 2.5 and 5 MV/m per nominal gradient of 25 MV/m. Significant beam blow-up and orbit distortion is only seen in the last of these cases.